Experimental and numerical investigation on thermoelectric coolers for comparing air-to-water to air-to-air refrigerators

Faraz Afshari[1]

Abstract

It has been determined that a significant portion of the total electrical energy is consumed for different cooling and refrigeration purposes at both domestic and industrial sectors. Moreover, cooling systems are employed in a wide range of critical fields such as food industry and pharmacy. In this study, experimental and numerical approach to evaluate two different modes of thermoelectric cooler efficiency is presented. Portable thermoelectric refrigerators operated by Peltier element have been constructed, and experiments are conducted to compare efficiency of air-to-water and air-to-air thermoelectric coolers. In air-to-air mode, the Peltier device was united with heat sinks and fans on both sides. However, in air-to-water mode, a water pump and suitable water-cooled heat exchanger were used to operate in the refrigerators made of styrofoam sheets. It was revealed that, in the laboratory conditions, air-to-water mode is more efficient than air-to-air mode and COP value of the air-to-water is approximately 30–50% higher than that of air-to-air refrigerator. Moreover, ANSYS Fluent 16.0 software has been used to analyze the problem closely in detail. The problem has been simulated, and CFD results were used to visualize flow structure and heat transfer characteristics inside refrigerator box.

Keyword Thermoelectric coolers · Peltier effect · Cooling capacity · COP · CFD

List of symbols

COP Coefficient of performance
C_p Specific heat capacity ($J\ kg^{-1}\ K^{-1}$)
CFD Computational fluid dynamics
I Electric current (A)
K Device thermal conductance ($W\ K^{-1}$)
$\dot{m}$ Mass flow rate ($kg\ s^{-1}$)
m Mass (kg)
P Pressure ($N\ m^{-2}$)
$\dot{Q}$ Heat transfer rate (W)
Q Heat transfer (J)
t Time (s)
T Temperature (°C)
u Velocity ($m\ s^{-1}$)
v Volume (m^3)
V Voltage (V)
W Power consumption (W)
TE Thermoelectric
ρ Density ($kg\ m^{-3}$)

μ Dynamic viscosity ($kg\ m^{-1}\ s^{-1}$)
α Seebeck coefficient ($V\ K^{-1}$)

Subscripts

c Cold side
fa Fan
h Hot side
Pe Peltier
Pu Water pump

✉ Faraz Afshari
faraz.afshari@erzurum.edu.tr; faraz.afshari@atauni.edu.tr

[1] Department of Mechanical Engineering, Erzurum Technical University, 25240 Erzurum, Turkey

Introduction

Preserving fresh foods and vegetables in clean and appropriate conditions is an important issue for human health. Generally, vapor compression refrigerator has been used for cooling applications in homes and supermarkets. But the large size of vapor compression refrigerator limits its application in small and temporary places.

Utilizing thermoelectric cooling system can be a good alternative for vapor compression refrigerator because of its several advantages. Thermoelectric refrigerators have low energy efficiency in comparison with traditional refrigerators. However, their rapid thermal response, long lifetime, high reliability, silent operation, having no fluid with

environmental impact, lightweight and compact structure make them attractive to use as mini-refrigerator for preserving foods and drugs in small places and also as a portable refrigerator. In addition, thermoelectric refrigerators can be a good solution for people living in refugee camps. Furthermore, the thermoelectric device can be used in different applications such as generating electricity from waste heat, cooling electronic components and air-conditioning [1]. The Peltier effect is also utilized in thermal analysis, heat flow compensation, calorimetry and calibration. Cooling devices on the Peltier effect are used for the design and manufacturing of isothermal microcalorimeters and PC processors [2].

In the literature, thermoelectric systems have been investigated by many researchers with regard to energy efficiency and optimum working conditions. The optimum input electrical current was specified in a wide range of heat loads by Chang et al. [3]. In another study, thermoelectric materials, applications, modeling approaches were reviewed and TE cooling applications including electronic cooling systems, domestic refrigeration and automobile air-conditioning were discussed [4]. Compression vapor heat pump and refrigerator system were evaluated for increasing their efficiency by means of thermoelectric generation using compressor heat losses [5]. Thermal balance equations were developed to find out TE performance using analytical solutions by Zhang [6]. Yin et al. investigated the effect of adding thermoelectric generator on the performance of four different photovoltaic cells, including monocrystalline silicon, polycrystalline silicon, amorphous silicon and polymer photovoltaic cell. They indicated that increasing the thermal resistance of thermoelectric can remarkably enhance the performance of the system [7].

Efficient heat transfer, as one of the first-order problems in the field of cooling-heating systems and other industrial processes, is a title for many researches in the literature [8–10]. Mixed convection heat transfer as an advanced method was used to enhance heat transfer rate of water-based nanofluids in microchannel [11]. Mini-channel water-cooled thermoelectric refrigerator was studied, and COP value of the system was obtained in different flow rates and voltages over the time by Gokcek et al. [12]. A prototype domestic TE refrigerator was investigated to evaluate the system performance in terms of the coefficient of performance and cooling rate [13]. Two-stage thermoelectric coolers were used to increase the cooling capacity and COP value of TECs, and the applied electrical current was optimized by Cheng et al. [14]. In another study, a mini-thermoelectric refrigerator was manufactured using Peltier element to obtain optimum working conditions. Refrigerator box was equipped with Peltier–fans combination on both sides. The obtained results showed that optimum ambient temperature is 293 K. Also, COP reduces from 0.351 to 0.011 when the temperature of the cooled space decreases from 293 to 254.8 K [15]. Tan et al. theoretically analyzed a thermoelectric cooling system by using the thermodynamic second law to achieve the optimal working conditions. They investigated the effects of different parameters like electric current, thermal conductivity and cooling temperature on the system performance. From the results, it was indicated that cooling temperature was the most significant parameter affecting thermoelectric cooling system performance [16]. Modified pulse operation of thermoelectric for building cooling application was numerically investigated by Manikandan et al. The thermoelectric cooling system was analyzed by applying different cooling load, variable pulse current ratio, variable pulse width and dissimilar pulse shapes. The findings showed that modified pulse operation could enhance the cooling rate and COP by 23.3% and 2.12% in comparison with normal mode of operation [17]. Enescu et al. designed and simulated a thermoelectric refrigerator powered by solar photovoltaic cells and electric storage system [18]. Dimri et al. developed a thermal model for semitransparent photovoltaic thermal system equipped with thermoelectric. Their results showed that adding thermoelectric device to the semitransparent photovoltaic system increased the electrical efficiency by 7.266% [19]. Wang et al. used miniaturized thermoelectric device for microprocessors chip cooling. They experimentally and numerically investigated the effects of using this cooling system on microprocessors performance. The importance of thermal contact resistance was revealed, and it was shown that a higher thermal contact resistance needs a larger mini-contact to obtain optimum performance [20].

Moazzez et al. developed an experimental and numerical study to use thermoelectrics as a choice for air-conditioning inside the cars. It was revealed that the regulation in the layout of the heat sinks can improve the performance of the system [21]. The phase-change material has been integrated at the hot side of the thermoelectric cooler to maintain constant and relatively low temperature. This technique was used to increase thermal performance of the thermoelectric cooler. Variable geometric parameters of the heat sink, variable input currents to the TEC and variable cooling load conditions with different phase-change materials were investigated. The results showed that, with the use of phase-change material, temperatures of the thermoelectric cooler are reduced in both hot and cold sides [22].

The main objectives of this study are analyzing the effects of using different heat sink and comparing cooling performance of air-to-air and air-to-water modes. In this regard, three different size prototype thermoelectric refrigerators were manufactured and tested in different working conditions. CFD as a widespread method is a branch of fluid mechanics that uses numerical analysis to simulate engineering and industrial problems that involve fluid flows [23, 24]. In this work, the problem was also simulated with regard to extensive theoretical considerations established with the

support of CFD software to analyze air flow structure and thermal behavior of the refrigerators.

Experimental setup and test procedure

Thermoelectric modules are also considered as energy converters consisting of a bunch of thermocouples electrically connected in series. They are made of two different semiconductors that produce a thermoelectric cooling effect when a voltage is applied in the appropriate electric direction. Thermoelectric modules generally operate with two exchangers attached to their cold and hot sides in order to enhance heat transfer and increase performance of the system. In this study, three different sizes of laboratory refrigerator boxes manufactured of styrofoam sheets were used to examine the Peltier cooling performance in different working conditions. A, B and C box capacities are $15 \times 15 \times 15$, $20 \times 20 \times 20$ and $30 \times 30 \times 30$ cm respectively. In all three boxes, air-to-water and air-to-air modes were tested experimentally and obtained results have been compared. Schematic views and pictures of the refrigerators are shown in Fig. 1. The temperature variations were measured with T-type thermocouples, and the average temperature of the box was obtained. Electrical power consumption was also calculated by recorded current and voltage values obtained by using voltage/ampere meter
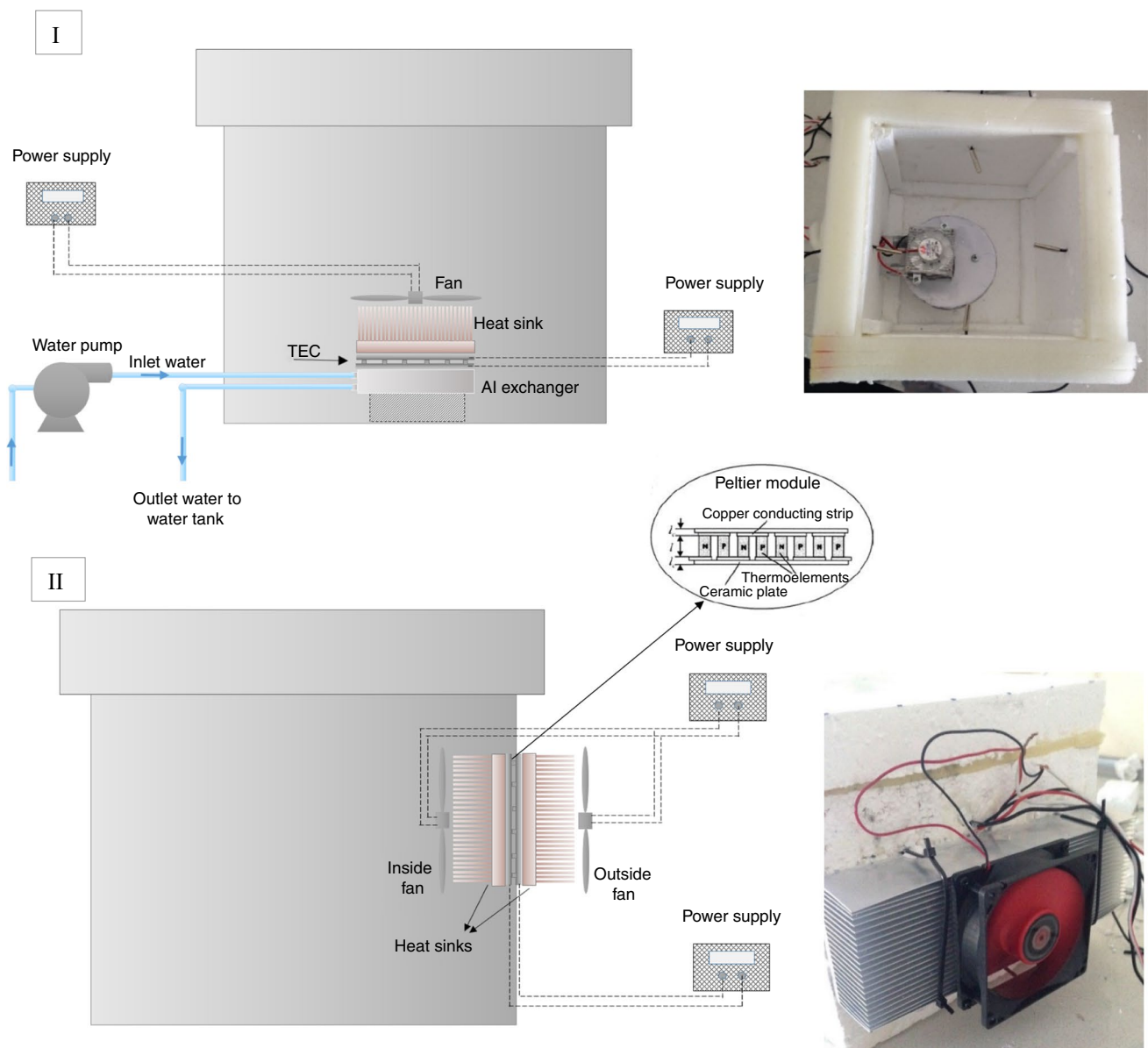

Fig. 1 Pictures and schematic views of air-to-water (I) and air-to-air (II) experimental setup

device. For air-to-air mode, two different 12-V DC fans were employed to provide forced convection heat transfer.

In the air-to-water mode, however, a water pump and suitable water-cooled heat exchanger attached to the hot side of thermoelectric Peltier were used. The most important part of the system consists of a thermoelectric Peltier, which features are presented in Table 1. Features of used water pump and heat exchanger have been also presented, respectively.

The processing flow diagram of experimental and numerical methods is shown in Fig. 2.

Analysis

Experimental analysis

Generally, in scientific studies on thermoelectric refrigerators, performance calculations can be made by two different methods.

In the first method, analysis starts with the prediction of the thermoelectric cooling and heating power. By assuming constant thermal and electrical properties of thermoelectric,

cooling power at the TEC cold side and heat transfer amount at hot side (Q_c and Q_h) can be expressed as (Chang et al. 2009),

$$Q_c = \alpha T_c I - \frac{1}{2}\left(I^2 R\right) - K\left(T_h - T_c\right) \tag{1}$$

$$Q_h = \alpha T_h I - \frac{1}{2}\left(I^2 R\right) - K\left(T_h - T_c\right) \tag{2}$$

COP value of the thermoelectric material can be expressed as,

$$(COP)_{c,max} = \frac{T_c}{T_h - T_c}\frac{\sqrt{1 + ZT_m} - \frac{T_h}{T_c}}{\sqrt{1 + ZT_m} + 1} \tag{3}$$

where ZT_m is the thermoelectric material figure of merit at average hot and cold side temperature T_m.

In the second method used in the present study, power consumption of the Peltier, water pump and fan should be taken into consideration and so the total COP value of the system can be written as follows,

Table 1 Peltier thermoelectric, water pump and heat sink features

Model	Operating voltage	Operating current	I_{max} (A)	Dimensions	Q_{max} (W)
Peltier thermoelectric features					
TEC1-12,715	12 V	<3 A	15 A	40×40×4 mm	231 W

Model	Operating voltage	Operating current	Flow rate	Dimensions	Diameter of hose connection	Maximum pressure
Water pump features						
SKU 50,200	12 V DC	<320 mA	0.02 kg/s	D27×75 mm	6.5 mm	360 mmHg

Model:	Heat sink material	Power	Dimensions	Bottom plate thickness	Tooth thickness	Number of teeth
Heat sink features						
FLE-CO0208	Aluminum	5.1 W	200×70×35 mm	4.6 mm	1.0 mm	27

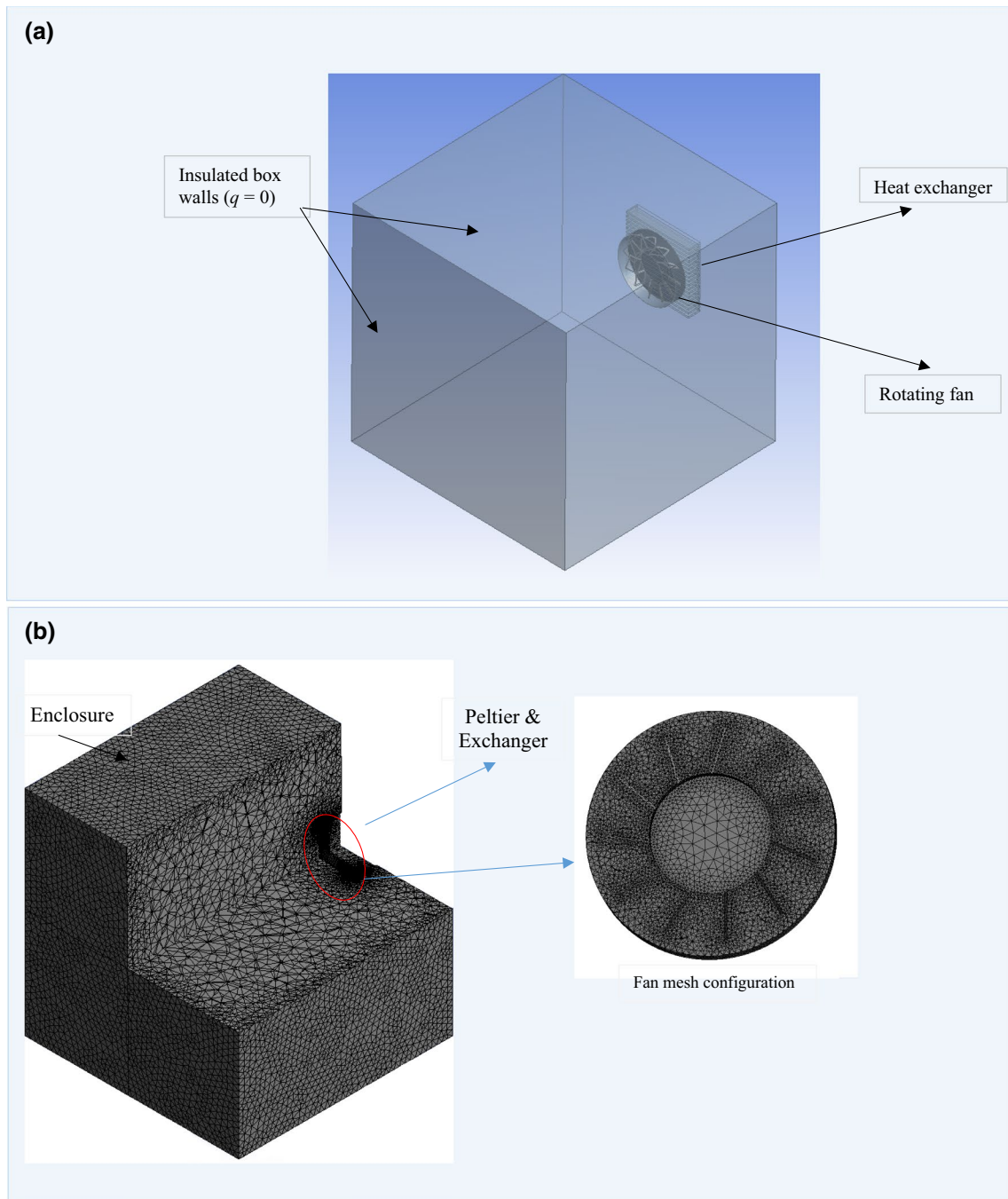**Fig. 2** Overall numerical and experimental processing flow diagram
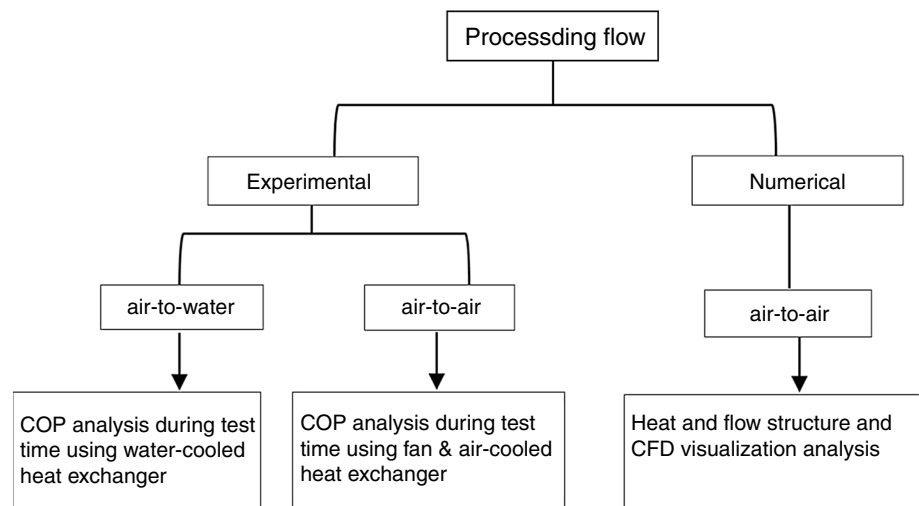
Fig. 3 Boundary conditions and domain extends (**a**) and schematic view of the mesh quality of refrigerator box, fan and exchanger (**b**)

$$\text{COP}_{\text{Tot}} = \frac{Q_{\text{c}}}{W_{\text{pe}} + W_{\text{fa}} + W_{\text{Pu}}} \tag{4}$$

On the other side, the amount of absorbed heat from the enclosed environment can be calculated by the following equation,

$$Q_{\text{c}} = mC_{\rho,\text{air}}\left(T_2 - T_1\right) \tag{5}$$

where T_2 and T_1 are the first and last temperatures of the refrigerator box and m is the air mass inside box. The mass of air contained in the refrigerator box can be obtained from the volume of the refrigerator box and the density of the air.

$$m = \rho v \tag{6}$$

Consumed electrical power can be calculated from recorded current and voltage values as,
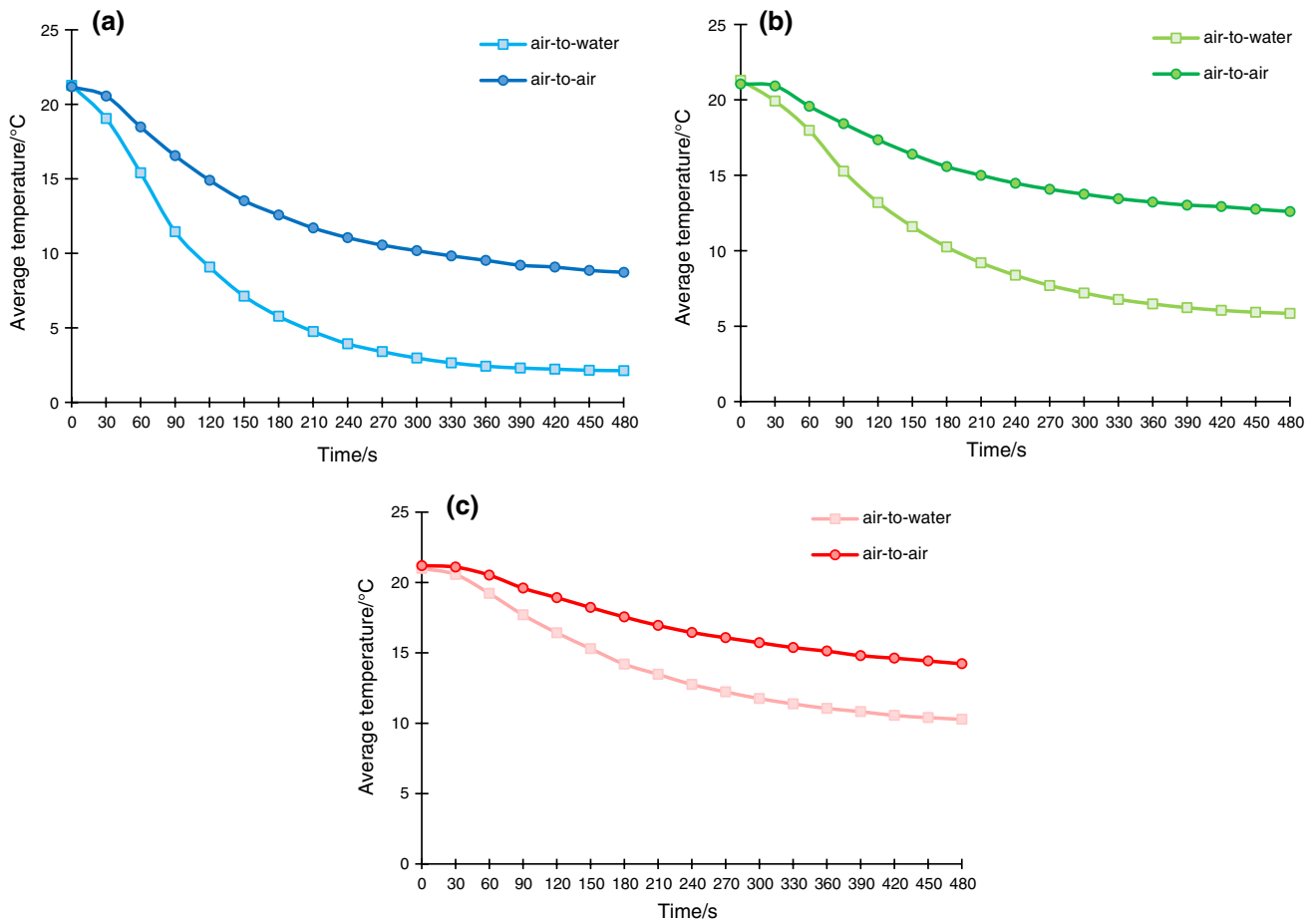
Fig. 4 Temperature of refrigerator boxes (A, B and C) with respect to test time at two modes (air-to-water and air-to-air)

$$W = IV \times (t) \tag{7}$$

Heat transfer by water in the air-to-water mode can be can be expressed as,

$$Q = \dot{Q} \times t = \left(\dot{m} C_{\rho,\text{wat}} \left(T_2 - T_1 \right) \right) \times t \tag{8}$$

CFD analysis

Simulation of engineering problems is a widespread method, frequently utilized to provide a holistic comprehension opportunity, accurate prediction and comparing to real situation. Simulation is also a scenario that closely mimics mechanical situations as well as other physical situations, which generally merges theory with actual perspectives and often provides insight into expected behaviors. In this study, ANSYS Fluent 16 as a CFD software is used to solve the problem and to meaningfully describe the flow structure and thermal behavior in the thermoelectric refrigerator box.

The model has been solved in transient state by using the mesh motion method to operate rotational movement of fan blades. SIMPLE second-order pressure, second-order upwind discretization scheme for energy, momentum, dissipation rate and turbulent kinetic energy were applied to solve the model. In this study, time step size of 0.03 s and max iterations/time step of 40 were defined to obtain heat transfer and temperature distribution over the solution time. The boundary condition of the present study is demonstrated in Fig. 3a.

Here, basic conservation equations in differential form have been presented as follows [33].

Mass conservation;

$$\frac{\partial \rho}{\partial t} + \nabla.(\rho \boldsymbol{u}) = 0 \tag{9}$$

Momentum equation;

$$\frac{\partial \rho \boldsymbol{u}}{\partial t} + \nabla.(\rho \boldsymbol{uu}) = -\nabla \mathrm{p} + \nabla.\left(\overline{\overline{\tau}} \right) + \rho \boldsymbol{g} + \mathbf{F} \tag{10}$$
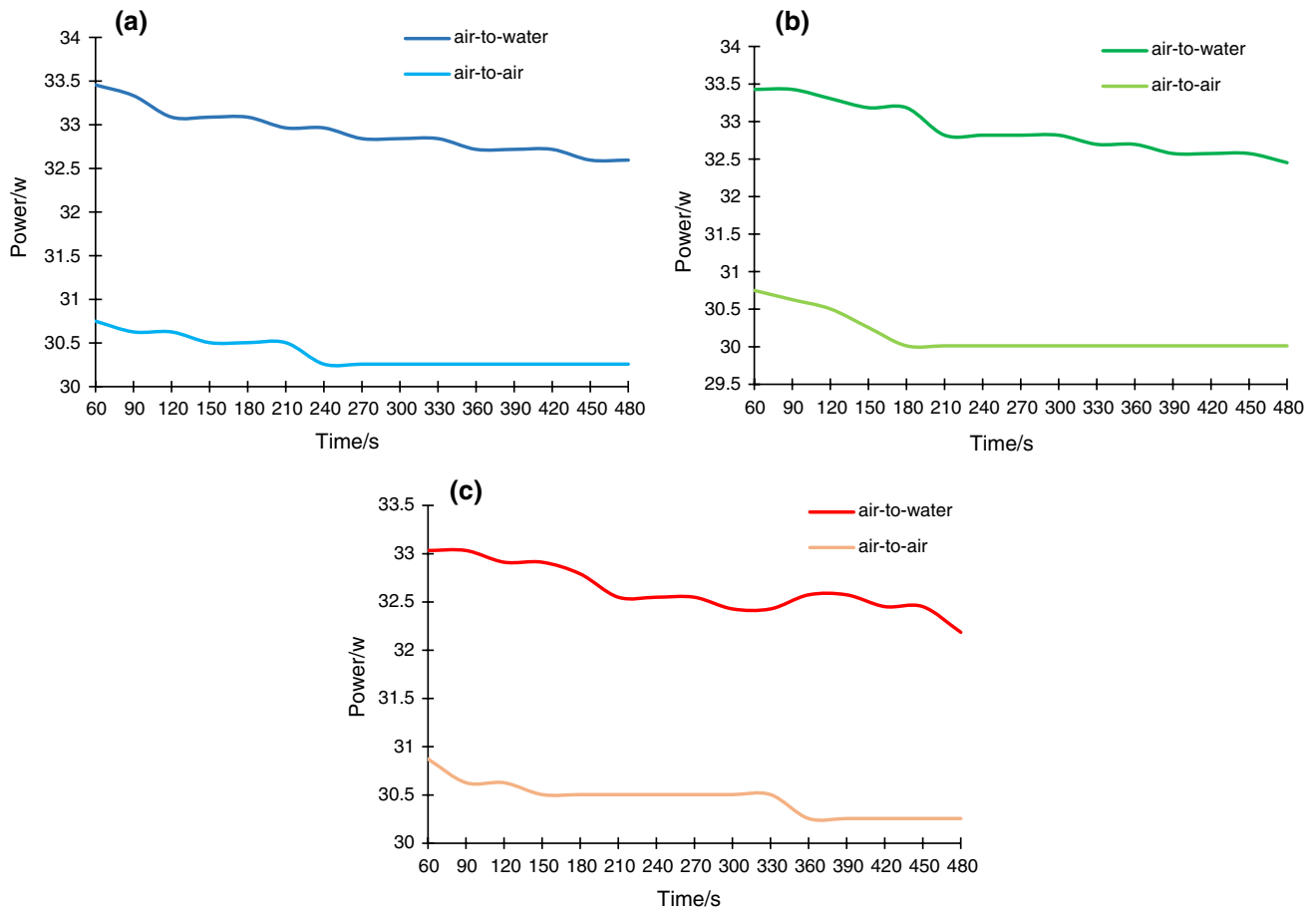
Fig. 5 Power consumption results of test boxes (A, B and C) in two modes

where p is the static pressure, $\overline{\overline{\tau}}$ is the stress tensor ρg and F are gravitational body force and external body forces.

Energy conservation;

$$\frac{\partial}{\partial t}(\rho E) + \nabla \cdot (\boldsymbol{u}(\rho E + p)) = \nabla \cdot \left(k_{\text{eff}} \nabla T - \sum_j h_j \boldsymbol{J}_j + \left(\overline{\overline{\tau}}_{\text{eff}} \cdot \boldsymbol{u} \right) \right) + S_{\text{h}}$$

(11)

where k_{eff} is the effective conductivity, J is diffusion flux of species and S_{h} is volumetric heat source. $k-\varepsilon$ Realizable model is one of the most used solution models in numerical methods which is also used in the present work as follows:

$$\frac{\partial}{\partial t}(\rho k) + \frac{\partial}{\partial x_i}(\rho k u_i) = \frac{\partial}{\partial x_j}\left[\left(\mu + \frac{\mu_t}{\sigma_k}\right)\frac{\partial k}{\partial x_j}\right]$$
$$+ G_k + G_b + S_k - Y_M - \rho\varepsilon$$

(12)

$$\frac{\partial}{\partial t}(\rho\varepsilon) + \frac{\partial}{\partial x_i}(\rho\varepsilon u_i) = \frac{\partial}{\partial x_j}\left[\left(\mu + \frac{\mu_t}{\sigma_\varepsilon}\right)\frac{\partial f}{\partial x_j}\right]$$
$$+ C_{1\varepsilon}\frac{\varepsilon}{k}C_{3\varepsilon}G_b + S_\varepsilon + \rho C_1 S\varepsilon - \rho C_2 \frac{\varepsilon^2}{k + \sqrt{v\varepsilon}}$$

(13)

where

$$C_1 = \max\left[0.43, \frac{\eta}{\eta + 5}\right] \quad \eta = S\frac{k}{\varepsilon} \quad S = \sqrt{2S_{ij}S_{ij}}$$

(14)

G_k represents the generation of turbulence kinetic energy due to the mean velocity gradients, G_b is the generation of turbulence kinetic energy due to buoyancy, Y_M represents the contribution of the fluctuating dilatation in compressible turbulence to the overall dissipation rate, and $C_{1\varepsilon}$ and C_2 are constants. In Fig. 3a, b schematic view of the mesh configuration is displayed where the analysis domain has been defined. In order to increase the accuracy of the calculations and reduce the error rate, various revisions in mesh generation and problem solving are required. In this study, mesh analysis has been performed to select optimum mesh number, cell types and sizes. Curvature mode and triangle
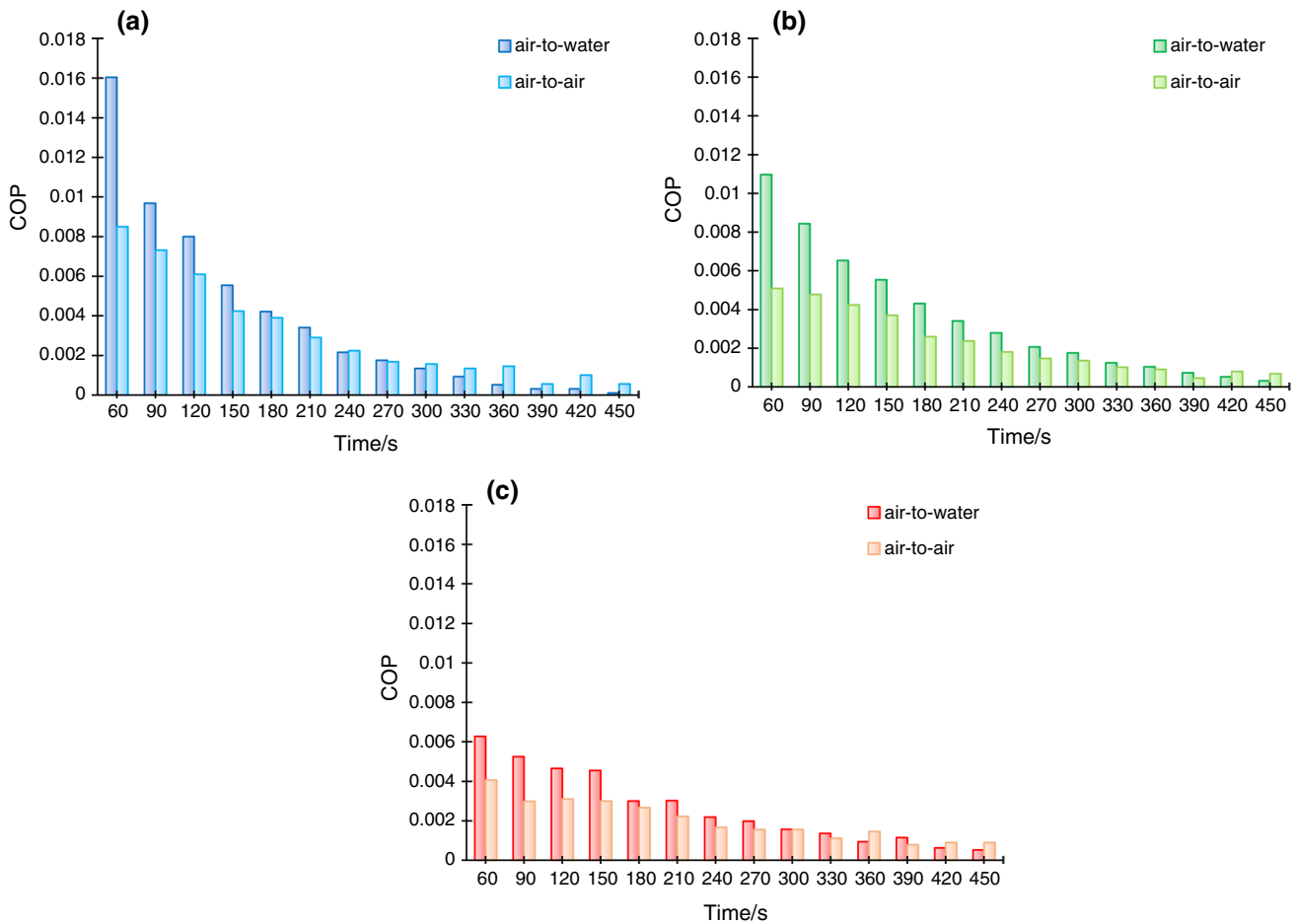
Fig. 6 COP results of A, B and C boxes versus test time for air-to-water and air-to-air modes
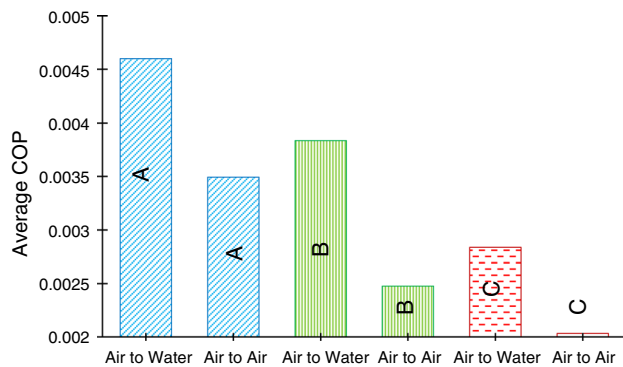

Fig.7 Average COP results of test boxes (A, B and C) in two modes

mesh surface were selected with growth rate of 1.2 and maximum face size of 1.295×10^{-2} m. Skewness value was also checked in the mesh generation process; average and maximum skewness values in the solution are about 0.26 and 0.80, respectively.

Results and discussion

Experimental results

In this work, planned experiments with different box sizes (A, B and C) were conducted to determine and compare the performance of thermoelectric materials in two different modes including air-to-air and air-to-water modes. The internal temperature of the boxes was recorded during experiments, and the average temperature obtained from the thermocouples was calculated.

Figure 4 represents the experimental results for temperature variation over the test time that is 480 s. The acquired results indicate that air-to-water state has the capability to decrease temperature faster, and lower temperatures can be achieved in this mode. It seems that, in larger boxes (like case C), one thermoelectric is insufficient to access lower temperature rapidly and so more Peltier devices should be used in the system.

In order to calculate the total COP values, the total amount of power consumed in the system should be

Table 2 A comparison of the results obtained in the present study with the literature

Reference	Refrigerator type	Refrigerator capacity	Power supply	Application field	COP	Results
Anyanwu, et al. [25]	Adsorption solar refrigerator	–	Solar energy	Prototype refrigerator	0.16–0.3	Carbon/methanol, carbon/ammonia and zeolite/water pairs was used as adsorbent/adsorbate, and the best result was obtained for zeolite/water pair
Afshari et al. [26]	Vapor compression	102×83×190 cm	Electrical energy	Prototype vapor compression refrigerator	0.051 (maximum)	COP of heat pumps and refrigerators was compared. The COP of refrigerators was very low compared to heat pumps
De Marchi Neto et al. (2009) [27]	Vapor compression	~337 L	Electrical energy	Conventional refrigerator	0.2–0.85	Waste heat in condenser successfully was used for hot water providing
Jugsujinda et al. [28]	Thermoelectric refrigerator	25×25×35 cm	20–40 W	Prototype refrigerator	0.65	The temperature of refrigerator was decreased from 30 to 20 °C in 1 h
Abdul-Wahab et al. [29]	Thermoelectric refrigerator	23×18×32 cm	9.5 W	Portable domestic refrigerator	0.16	Performance of system strongly depends on the temperature difference of cold and hot sides of thermoelectric
Mirmanto et al. [30]	Thermoelectric refrigerator	215×175×130 cm	38.08 W	Prototype refrigerator	0- 0.025	The thermoelectric was mounted on the wall, top and bottom. The best performance was obtained in the wall position
Mirmanto et al. [31]	Thermoelectric refrigerator	285×245×200 cm	1.04–38.76 W	Prototype cooler box	0–0.02	COP decreased by increasing power. But temperature difference increased by increasing power
Caglar [15]	Thermoelectric refrigerator	60×40×27 cm	Electrical energy	Prototype refrigerator	0.011–0.351	Optimum conditions for a thermoelectric refrigerator were investigated
Martinez et al. (2016)	Thermoelectric refrigerator	0.062 m³	Electrical energy	Prototype refrigerator	0.09–0.33	Computational model for Peltier effect-based refrigerators was examined
This study	Thermoelectric refrigerator	15×15×15 cm, 20×20×20 cm, 30×30×30 cm	30–35 W	Prototype refrigerator	0.017 (maximum)	COP reduced during test time. Air-to-water mode shows higher performance than air-to-air

Fig. 8 3D velocity volume-rendering results **a** 2D velocity contour, **b** and streamlines **c** inside refrigerator box A
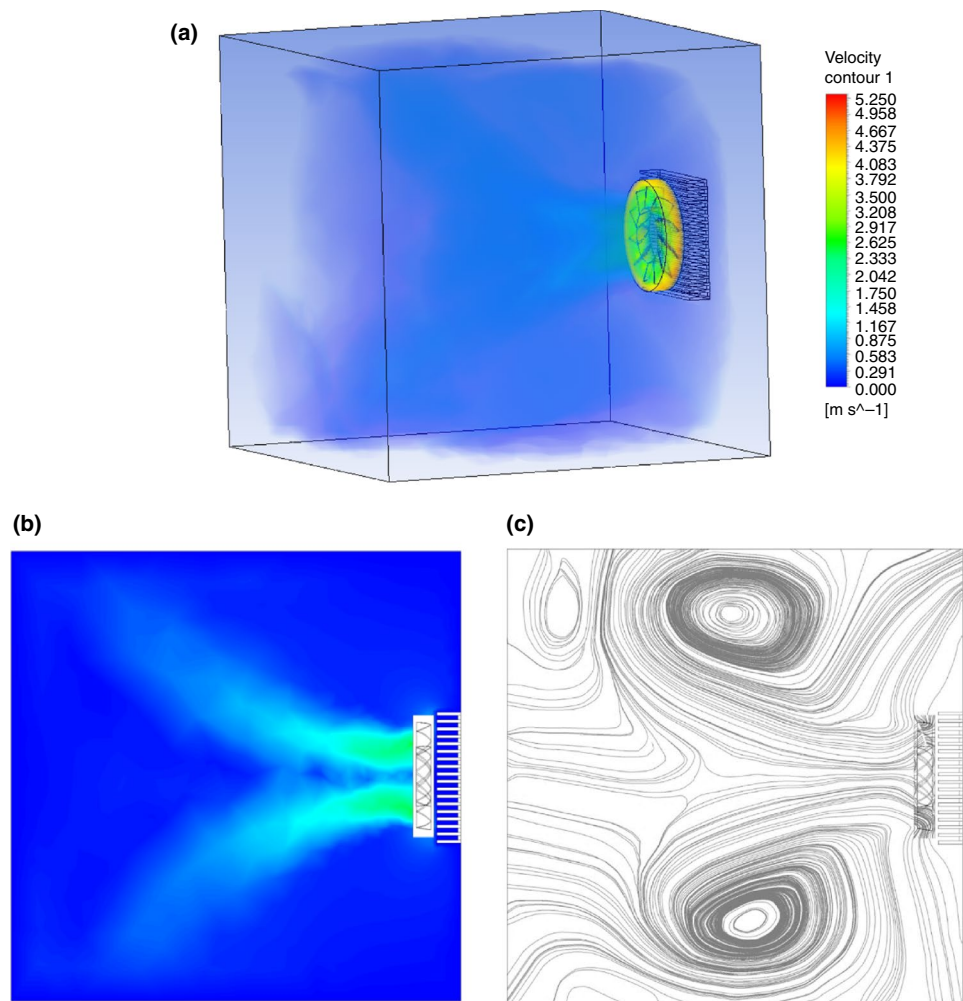
measured. The consumed electrical power was obtained from the continuously recorded voltage and current values using a digital volt-ampere meter. In all experiments, it was revealed that the power consumption in air-to-water was about 5–10% higher than air-to-air mode.

Furthermore, at the beginning of the experiments, the power consumption is at its highest point, but decreases gradually during time. In air-to-air mode, this value was decreased and fixed at the constant value toward the end of the test time. The power consumption values of all test boxes are given in Fig. 5 for both modes.

The corresponding COP results calculated from Eq. (8) for TEC system under air-to-water and air-to-air cooling conditions are shown in Fig. 6 for different test boxes. It was revealed that small box (A) has the maximum performance among test boxes due to lower heat losses and also at the beginning COP values of the air-to-water mode is noticeably higher than air-to-air mode.

However, its value decreases gradually over test time and becomes less than air-to-air mode at the end of the experiments.

The COP diagrams presented earlier in Fig. 6 showed that its value in the air-to-water mode is reduced toward the end of the test time and become less than those of air-to-air mode. This is because the air-to-water mode is able to draw faster thermal energy out of the box at the first seconds of this experiment. Furthermore, lower temperatures were obtained in the air-to-water mode during the test time, which is an indication of their higher effective operation. For better comparison, the average COP values were also compared in two modes for the A, B and C boxes presented in Fig. 7, which shows a 30–50% improvement in the air-to-water mode.

At the first step during the calculations and analysis of the obtained results, the low COP values of the refrigerator were thought outside of expectations and unreasonable and led to a criticism. However, after a thorough and basic screening and research on the literature results, it was observed that the COP value in the refrigerators and cooling devices is low and is not a constant value as heat pumps.

In refrigerators and cooling systems, the decline of COP over time has made it more difficult to compare different

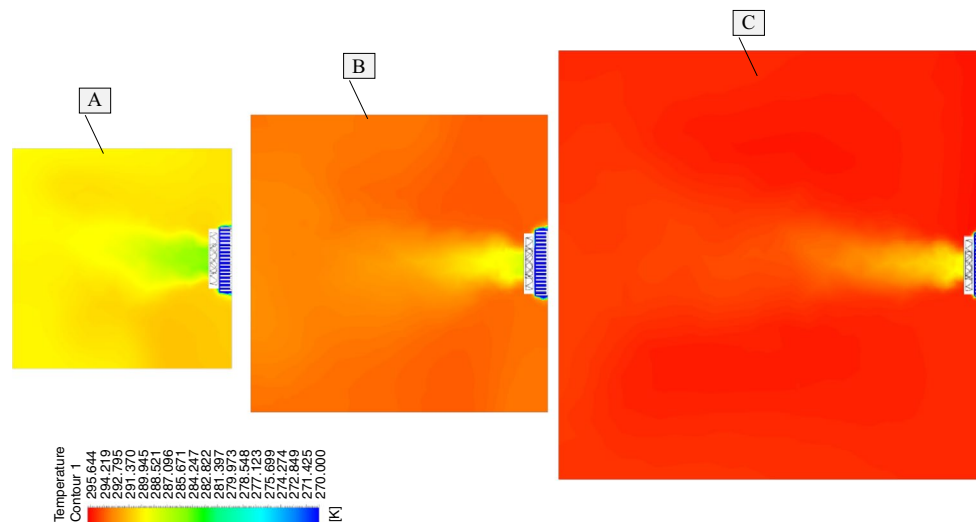**Fig. 9** Temperature distribution of refrigerator (A) in 5-s intervals
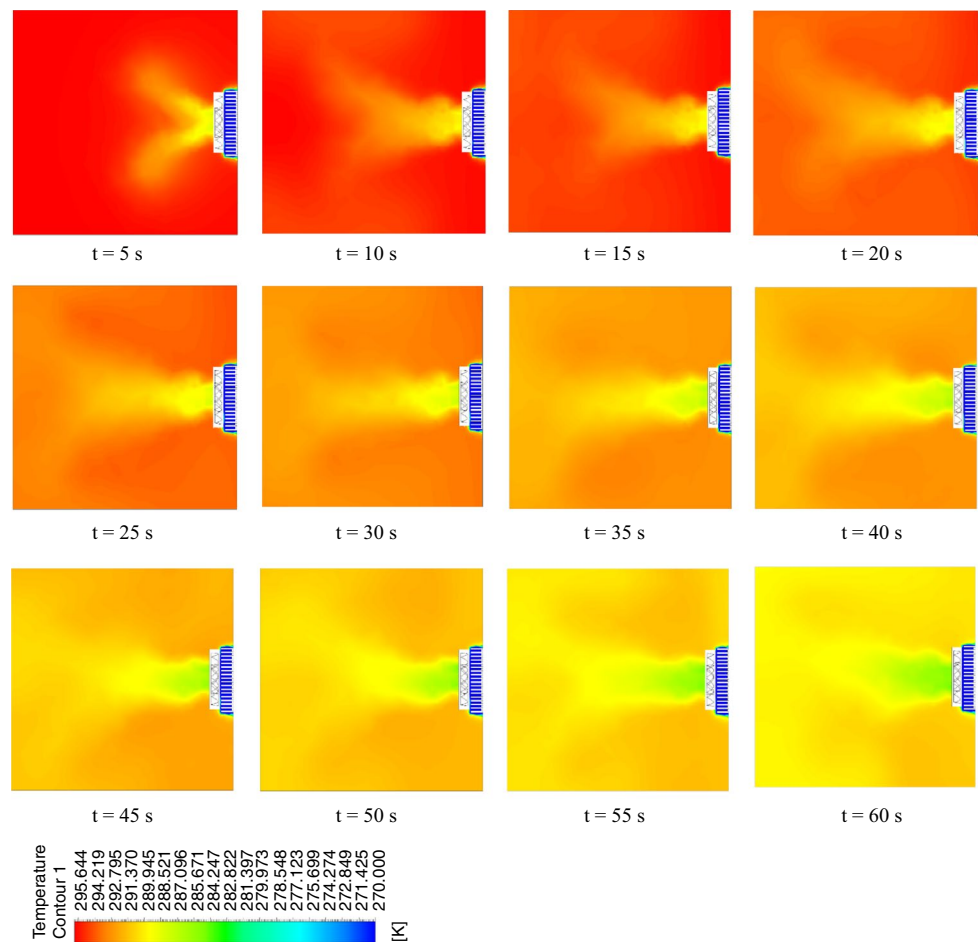
types of refrigeration devices. However, even if the COP value is low and inefficient for refrigerators, cooling purpose can be achieved with very little power consumption for quotidian cooling or freezing necessities. Generally, low COP values of refrigerators have been considered and partially discussed in the literature as shown in the form of a table (Table 2). The reason for this issue is that, in the refrigerators the thermal energy reserves are only available in a certain small volume on the evaporator side (unlike heat pumps and air-conditioning systems, which extract energy from large areas and thus benefit from a wider energy source). In particular, when the cooling process begins, the temperature of the refrigerator box begins to drop and the thermal energy levels inside volume is further fallen down and consequently the COP value decreases. Although this is more remarkable in Peltier cooling systems, these systems are becoming widespread because they are considerably lighter and easier to install.

CFD results

In this section, the velocity and temperature contours obtained from CFD solution are presented to survey flow structure and thermal behavior of the refrigerator over the cooling time.

In Fig. 8a, velocity volume-rendering methods are utilized in the first step to illustrate an overall three-dimensional visualization of the velocity and fluid flow of the model for smallest box (A). The interior space of the refrigerator, fan rotation and the air circulation is clearly indicated in the figure.

In Fig. 8b and c, two-dimensional velocity contour and streamlines inside air-to-air refrigerator box (box A) are also presented. From the velocity contour, it can be observed that a high-velocity region in front of the fan is created and consequently vorticity formation is likely to be occurred. In the next stage, formation of vortex in the flow structure is given in the streamlines configuration. The

Fig. 10 Temperature distribution of refrigerator boxes A, B and C at 60th second

number of streamlines and line width have been adjusted to make them easier to distinguish from each other on a central plane. Another important issue is that, streamlines configuration is slightly changed over the time and small vortex is appeared from time to time, but their general configuration is similar to that provided in Fig. 8c. In the present study, numerically obtained streamlines and velocity pattern can be surveyed experimentally using particle image velocimetry (PIV) system which is a high-cost technique and needs laboratory equipment.

In thermoelectric coolers, the Peltier effect is utilized to produce a heat flux at the junction of two different types of materials. Heat exchangers have an important role in this type of cooling systems. In order to enhance the heat transfer rate from hot and cold sides and also to increase the efficiency of the Peltier device, efficient heat exchangers are required on both sides. More importantly, a Peltier device operated without cooling applications on the hot side is exposed to an internal temperature increasing exponentially until the internal joins melt and consequently the device will quickly burn out. In Fig. 9, the temperature distribution for box A is shown at 12 steps in 5-s intervals. According to CFD results, in the cooling trend, the role of Peltier thermoelectric and heat exchanger in extracting thermal energy from refrigerator box is clearly shown. In the presence of an exchanger and fan, convective heat transfer mechanism has been activated and low-temperature air flow separates from exchanger and approaches the high-temperature zone and this process causes the thermal energy to be evacuated from the refrigerator.

Within the same period and at the end of stage 12 (60th second), temperature distribution of all boxes (A, B and C) is presented in Fig. 10. In other words, the final contour in Fig. 9 was also provided for boxes B and C, and the results of all boxes are compared in Fig. 10.

As shown in the figure, cooling process of the smallest box in volume (A) is considerably quick compared to other boxes, which shows a good agreement with the experimental results. It can be observed that, in larger boxes, if more rapid cooling is desired, more Peltier thermoelectric should be employed.

Conclusions

In this work, different sizes of cube boxes were made using styrofoam sheets and Peltier thermoelectric efficiency was examined for air-to-air and air-to-water experimental sets in laboratory conditions. In air-to-air mode, two heat exchangers and two fans were attached on hot and cold surfaces. In the air-to-water mode, the fan and heat exchanger of the cold surface were the same, but a water-cooled exchanger was used instead of the fan on the hot surface, and the values obtained from the two modes were compared.

In this study, it was observed that the average COP value of air-to-water mode is approximately 30–50% higher than that of air-to-air mode. In other words, air-to-water thermoelectric cooling device operates more efficiently. In addition, the COP values of the refrigerators calculated by the thermodynamic method were

compared with several research in the literature. However, the obtained COP results are very low in contrast to heat pumps.

In addition, ANSYS Fluent software was used to simulate the problem and required contours were prepared to survey heat and fluid flow characteristics inside refrigerator box.

Compliance with ethical standards

Conflict of interest The author declares that there is no conflict of interest.

References

1. Tan FL, Fok SC. Methodology on sizing and selecting thermoelectric cooler from different TEC manufacturers in cooling system design. Energy Convers Manage. 2008;49(6):1715–23. https://doi.org/10.1016/j.enconman.2007.11.001.
2. Drebushchak VA. The peltier effect. J Therm Anal Calorim. 2008;91(1):311. https://doi.org/10.1007/s10973-007-8336-9.
3. Chang YW, Chang CC, Ke MT, Chen SL. Thermoelectric air-cooling module for electronic devices. Appl Therm Eng. 2009;29(13):2731–7. https://doi.org/10.1016/j.applthermaleng.2009.01.004.
4. Zhao D, Tan G. A review of thermoelectric cooling: materials, modeling and applications. Appl Therm Eng. 2014;66(1–2):15–24. https://doi.org/10.1016/j.applthermaleng.2014.01.074.
5. Navarro-Peris E, Corberan JM, Ancik Z. Evaluation of the potential recovery of compressor heat losses to enhance the efficiency of refrigeration systems by means of thermoelectric generation. Appl Therm Eng. 2015;89:755–62. https://doi.org/10.1016/j.applthermaleng.2015.06.033.
6. Zhang HY. A general approach in evaluating and optimizing thermoelectric coolers. Int J Refrig. 2010;33(6):1187–96. https://doi.org/10.1016/j.ijrefrig.2010.04.007.
7. Yin E, Li Q, Xuan Y. Thermal resistance analysis and optimization of photovoltaic-thermoelectric hybrid system. Energy Convers Manage. 2017;143:188–202. https://doi.org/10.1016/j.enconman.2017.04.004.
8. Khanlari A, Sözen A, Variyenli Hİ. Simulation and experimental analysis of heat transfer characteristics in the plate type heat exchangers using TiO2/water nanofluid. Int J Numer Methods Heat Fluid Flow. 2018. https://doi.org/10.1108/HFF-05-2018-0191.
9. Khanlari A, Sözen A, Variyenli Hİ, Gürü M. Comparison between heat transfer characteristics of TiO2/deionized water and kaolin/deionized water nanofluids in the plate heat exchanger. Heat Transf Res. 2019;50(5):435–50. https://doi.org/10.1615/HeatTransRes.2018026288.
10. Solangi KH, Sharif S, Nizamani B. Effect of tube material on convective heat transfer of various nanofluids. J Therm Anal Calorim. 2019. https://doi.org/10.1007/s10973-019-08835-z.
11. Manay E, Mandev E. Experimental investigation of mixed convection heat transfer of nanofluids in a circular microchannel with different inclination angles. J Therm Anal Calorim. 2019;135(2):887–900. https://doi.org/10.1007/s10973-018-7463-9.
12. Gokcek M, Sahin F. Experimental performance investigation of minichannel water cooled-thermoelectric refrigerator. Case Stud Therm Eng. 2017;10:54–62. https://doi.org/10.1016/j.csite.2017.03.004.
13. Min G, Rowe DM. Experimental evaluation of prototype thermoelectric domestic-refrigerators. Appl Energy. 2006;83(2):133–52. https://doi.org/10.1016/j.apenergy.2005.01.002.
14. Cheng YH, Shih C. Maximizing the cooling capacity and COP of two-stage thermoelectric coolers through genetic algorithm. Appl Therm Eng. 2006;26(8–9):937–47. https://doi.org/10.1016/j.applthermaleng.2005.09.016.
15. Caglar A. Optimization of operational conditions for a thermoelectric refrigerator and its performance analysis at optimum conditions. Int J Refrig. 2018;96:70–7. https://doi.org/10.1016/j.ijrefrig.2018.09.014.
16. Tan H, Fu H, Yu J. Evaluating optimal cooling temperature of a single-stage thermoelectric cooler using thermodynamic second law. Appl Therm Eng. 2017;123:845–51. https://doi.org/10.1016/j.applthermaleng.2017.05.182.
17. Manikandan S, Kaushik SC, Yang R. Modified pulse operation of thermoelectric coolers for building cooling applications. Energy Convers Manage. 2017;140:145–56. https://doi.org/10.1016/j.enconman.2017.03.003.
18. Enescu D, Ciocia A, Mazza A, Russo A. Solutions based on thermoelectric refrigerators in humanitarian contexts. Sustain Energy Technol Assess. 2017;22:134–49. https://doi.org/10.1016/j.seta.2017.02.016.
19. Dimri N, Tiwari A, Tiwari GN. Thermal modelling of semitransparent photovoltaic thermal (PVT) with thermoelectric cooler (TEC) collector. Energy Convers Manage. 2017;146:68–77. https://doi.org/10.1016/j.enconman.2017.05.017.
20. Wang P, Yang B, Bar-Cohen A. Mini-contact enhanced thermoelectric coolers for on-chip hot spot cooling. Heat Transfer Eng. 2009;30(9):736–43. https://doi.org/10.1080/01457630802678391.
21. Fattahpour Moazzez A, Naja G, Ghobadian B, Hoseini S. Numerical simulation and experimental investigation of air cooling system using thermoelectric cooling system. J Therm Anal Calorim. 2019. https://doi.org/10.1007/s10973-019-08899-x.
22. Manikandan S, Selvam C, Praful PPS, Lamba R, Kaushik SC, Zhao D, Yang R. A novel technique to enhance thermal performance of a thermoelectric cooler using phase-change materials. J Therm Anal Calorim. 2019. https://doi.org/10.1007/s10973-019-08353-y.
23. Afshari F, Zavaragh HG, Sahin B, Grifoni RC, Corvaro F, Marchetti B, Polonara F. On numerical methods; optimization of CFD solution to evaluate fluid flow around a sample object at low Re numbers. Math Comput Simul. 2018;152:51–68. https://doi.org/10.1016/j.matcom.2018.04.004.
24. Abbaspour M, Radmanesh AR, Soltani MR. Unsteady flow over offshore wind turbine airfoils and aerodynamic loads with computational fluid dynamic simulations. Int J Environ Sci Technol. 2016;13(6):1525–40. https://doi.org/10.1007/s13762-016-0995-2.
25. Anyanwu EE, Ogueke NV. Thermodynamic design procedure for solid adsorption solar refrigerator. Renew Energy. 2005;30(1):81–96. https://doi.org/10.1016/j.renene.2004.05.005.
26. Afshari F, Comakli O, Karagoz S, Zavaragh HG. A thermodynamic comparison between heat pump and refrigeration device using several refrigerants. Energy Build. 2018;168:272–83. https://doi.org/10.1016/j.enbuild.2018.03.037.
27. De Marchi NI, Padilha A, Scalon VL. Refrigerator COP with thermal storage. Appl Therm Eng. 2009;29(11–12):2358–64. https://doi.org/10.1016/j.applthermaleng.2008.12.003.

28. Jugsujinda S, Vora-ud A, Seetawan T. Analyzing of thermoelectric refrigerator performance. Proced Eng. 2011;8:154–9. https://doi.org/10.1016/j.proeng.2011.03.028.

29. Abdul-Wahab SA, Elkamel A, Al-Damkhi AM, Ishaq A, Al-Rubai'ey HS, Al-Battashi AK, Chutani MU. Design and experimental investigation of portable solar thermoelectric refrigerator. Renew Energy. 2009;34(1):30–4. https://doi.org/10.1016/j.renene.2008.04.026.

30. Mirmanto M, Syahrul S, Wirdan Y. Experimental performances of a thermoelectric cooler box with thermoelectric position variations. Eng Sci Technol Int J. 2019;22(1):177–84. https://doi.org/10.1016/j.jestch.2018.09.006.

31. Mirmanto M, Sayoga IMA, Sutanto R, Alit IB, Nurchayati N, Mulyanto A. Experimental cooler box performance using two different heat removal units: a heat sink fin-fan, and a double fan heat pipe. Front Heat Mass Transf (FHMT). 2018. https://doi.org/10.5098/hmt.10.34.

32. Martinez A, Astrain D, Rodriguez A, Aranguren P. Advanced computational model for Peltier effect based refrigerators. Appl Therm Eng. 2016;95:339–47. https://doi.org/10.1016/j.applthermaleng.2015.11.021.

33. Afshari F, Zavaragh HG, Di Nicola G. Numerical analysis of ball-type turbulators in tube heat exchangers with computational fluid dynamic simulations. Int J Environ Sci Technol. 2019;16(7):3771–800. https://doi.org/10.1007/s13762-018-2012-4.